Simultaneous pH–rate profiles applied to the two step consecutive sequence $A \rightarrow B \rightarrow C$: a theoretical analysis and experimental verification †

John Andraos,*[a] Edward C. Lathioor[b] and William J. Leigh[b]

[a] *Department of Chemistry, University of Toronto, Toronto, ON M5S 3H6 Canada*
[b] *Department of Chemistry, McMaster University, Hamilton, ON L8S 4M1 Canada*

Received (in Gainesville, FL) 1st July 1999, Accepted 24th November 1999

The absorbance extremum method introduced to resolve the rate constant–reaction step ambiguity problem in two step consecutive reactions is applied to cases where the rate constant in each step is pseudo first order and dependent on catalyst concentration. In particular, acid and base catalyzed reactions of substrates in aqueous solution are examined. Resultant simultaneous pH–rate profile functions are treated in the context of the ambiguity problem and a detailed account of the possible interactions between pH–rate profiles is also given. The merits of this method include its general scope, its applicability to reactions for which it may be experimentally difficult to resolve the ambiguity assignment by other means, and its use of rate data acquired from original kinetic traces without requiring additional information. The theoretical analysis is verified and tested experimentally for the hydration of fluorenylideneketene in dilute aqueous perchloric acid solutions.

Introduction

The study of acid and base catalysis has been at the forefront of mechanistic investigations in physical organic chemistry. The founding principles of chemical reactivity and the mechanistic tools designed for probing reaction mechanisms have been established largely from investigations of acid–base catalyzed reactions of simple molecules.[1] Of particular interest to medicinal and pharmaceutical chemists are kinetic and product studies which track the degradation pathways of drug molecules or metabolites in living systems. In order to better understand these enzyme mediated reactions, it is useful to examine the corresponding non-enzymatic acid or base catalyzed reactions in aqueous solution. In practice the reaction of a substrate, usually an organic molecule, is examined under pseudo first order conditions where the concentrations of the possible catalysts in such media, hydronium ion and hydroxide ion, remain invariant with time during the course of the kinetics experiment. A central kinetic plot in these studies is the pH–rate profile which relates the variation of the observed pseudo first order rate constant with pH, a parameter which by definition is related to either hydronium ion or hydroxide ion concentration. The shapes of pH–rate profiles reveal insights about reaction mechanisms such as the existence of ionizable groups in the substrate, a change of rate limiting step in a mechanism, or a change of mechanism altogether.[2]

Of particular importance is the simple reaction mechanism composed of two consecutive irreversible steps as shown in Scheme 1. This represents the second most ubiquitous scheme encountered in chemical kinetics studies after simple irreversible and reversible reactions involving two species. The time dependent absorbances of all three chemical species are given by the well-known expressions (1a–c), where A_A^0 is the initial absorbance of A, and ε_A, ε_B, and ε_C are the absorption coefficients of A, B, and C, respectively.

$$A \xrightarrow{k_1} B \xrightarrow{k_2} C$$

Scheme 1

$$A_A = A_A^0 \exp[-k_1 t]$$

$$A_B = A_A^0 \left(\frac{\varepsilon_B}{\varepsilon_A}\right)\left(\frac{k_1}{k_1 - k_2}\right)\{\exp[-k_2 t] - \exp[-k_1 t]\} \quad \text{(1a–c)}$$

$$A_C = A_A^0 \left(\frac{\varepsilon_C}{\varepsilon_A}\right)\left\{1 - \frac{1}{k_1 - k_2}(k_1 \exp[-k_2 t] - k_2 \exp[-k_1 t])\right\}$$

A closer examination of the kinetic behaviour of intermediate B reveals a subtle insight; namely, that for a growth-decay function of the form of eqn. (1b) it is impossible to assign unambiguously the rate constant parameters to the particular steps in the reaction sequence solely on the basis of the results of a *single* data fit according to this equation. In chemical terms, a given growth-decay kinetic curve may correspond to either of two situations: (i) a fast formation of a strongly absorbing intermediate in the first step followed by its slow decomposition in the second step, or (ii) a slow formation of a weakly absorbing intermediate in the first step followed by its rapid decomposition in the second step. Hence, although the growth part of a growth-decay curve always corresponds to the faster reaction, it does not necessarily follow that it also corresponds to the first reaction in the sequence. This mathematical ambiguity has been documented before[3] and a comprehensive review[4] of the problem has appeared in which a new absorbance extremum method was introduced to resolve the impasse. The method is based on a comparative analysis of several kinetic traces in which the signal size of intermediate B is characterised as a function of catalyst concentration such as hydronium ion.

† Table S1 giving all possible interactions between two pH–rate profiles; Tables S2 and S3 giving the rate data for the hydration of fluorenylideneketene and the ketonization of fluorene-9-carboxylic acid enol in aqueous perchloric acid solutions; Tables S4 and S5 giving the numerical data for implementing the absorbance extremum method; and Table S6 giving the numerical data for implementing the absorption coefficient method are available as supplementary data. For direct electronic access see http://www.rsc.org/suppdata/p2/a9/a905324g/, otherwise available from BLDSC (SUPPL. NO. 57689, pp. 15) or the RSC Library. See Instructions for Authors available *via* the RSC web page (http://www.rsc.org/authors).

This paper investigates the kinetic behaviour of chemical species *A*, *B*, and *C* when both k_1 and k_2 represent pseudo first order rate constants that are functions of pH as would be the case in pH–rate profiles. When these functions are plotted on the same graph there are necessarily several kinds of interactions that are possible between the two. These fall into the general classes of crossings, avoided crossings, complete overlap, partial overlap, and no overlap. A detailed analysis of simultaneous pH–rate profiles is presented in which all of these possible interaction conditions are considered. For each case, it will be shown how the absorbance extremum method can be used to unambiguously assign rate constant parameters from data fits to their appropriate steps in the reaction sequence.

In order to test the utility of this method in resolving the rate constant–reaction step ambiguity in the context of simultaneous pH–rate profiles, the hydration of fluorenylideneketene in aqueous perchloric acid solutions was chosen. This chemical system shown in Scheme 2 has been studied previously[5] and the

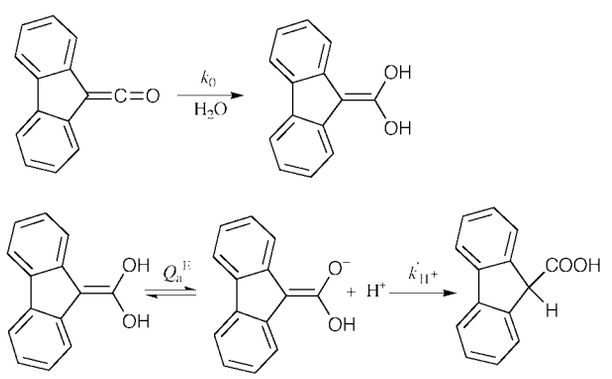

Scheme 2

pH–rate profiles for ketene hydration and enol ketonization have been well determined. This scheme follows exactly the pattern of two consecutive reactions shown in Scheme 1 with the labels *A*, *B*, and *C* referring to the ketene, enol in both ionized and unionized forms, and carboxylic acid species, respectively. Over the range of perchloric acid concentrations 0.0001 M to 0.1 M the reaction dynamics of intermediate fluorene-9-carboxylic acid enol were observed as growth-decay traces. Analysis of these kinetic traces allowed the construction of pH–rate profiles for ketene hydration and enol ketonization. Their assignments were made by comparing the rate data with the respective shapes of pH–rate profiles for the hydration and ketonization of known ketene and enol species in aqueous solution. It was found that the rate constant for ketene hydration to form the carboxylic acid enol, k_0, was independent of hydronium ion concentration and had a value of 1.07×10^5 s^{-1}. On the other hand, the subsequent ketonization step was strongly catalyzed by acid in dilute solutions and then exhibited saturation behaviour at high acid concentrations. From this kinetic behaviour the hydronium ion catalytic coefficient, k_{H^+}', and the equilibrium constant, Q_a^E, expressed as a concentration dissociation constant applicable to ionic strength 0.1, for the enol ionizing as an oxygen acid were determined to be 1.25×10^8 M^{-1} s^{-1} and 9.87×10^{-3} M, respectively. Based on the above experimental observations the pH-rate profile for hydration of fluorenylideneketene in acidic solutions was found to be a horizontal line consistent with the observation of no catalysis by hydronium ion; whereas, that for ketonization of fluorene-9-carboxylic acid enol was found to consist of two segments: a line of slope minus one in dilute acid and another of slope zero at high acid concentration. A plot showing both profiles simultaneously revealed that they intersected at about 0.002 M $HClO_4$. All of this evidence taken together allowed the growth and decay portions of the kinetic traces to be assigned to each reaction step. Hence, for acid solutions less than 0.002 M the growth portions of the traces corresponded to ketene hydration (step 1) and the decay portions to enol ketonization (step 2); whereas, for acid solutions greater than 0.002 M the former assignments were reversed.

The previous work was based on acquired kinetic traces that were optimized to give the best possible estimates of rate constants without paying any attention to the observed decrease of signal size with increasing acid concentration. Furthermore, previous knowledge of kinetic behaviours of other ketene and enol systems was essential in assigning rate constants in Scheme 2. We now report a method of arriving at the same assignments based on this signal size variation and which does not rely on any other data beyond the original kinetic traces obtained in our flash photolysis experiments. A background analysis of pH–rate profiles in the context of the rate constant–reaction step ambiguity problem is presented first and then it is shown how the above assignments may be made *a priori* in this chemical system using the absorbance extremum method. The assignments made in this chemical system are further supported when the method of absorption coefficients introduced by Alcock and co-workers[3a] is also applied to the rate data. This chemical system is ideal for verifying and testing all available methods for resolving the rate constant–reaction step ambiguity problem. The generality of the new method is emphasised in studies of sequential reactions.

Theoretical analysis

pH–rate profile functions

For the purpose of review, Table 1 summarizes the possible functions for a pseudo first order rate constant according to mode of catalysis, variation with pH, and limiting slopes. A pH–rate profile spanning the entire range in pH is conveniently described as a sum of any one or more of the elementary functions listed in Table 1. More precisely, a general pH–rate profile is given by eqn. (2), where the logarithm is taken to base

$$\log k_{obs} = \log\left[\sum_j f_j([H^+])\right] \qquad (2)$$

10 and $f_j([H^+])$ represents catalytic functions in terms of hydronium ion concentration.

There are essentially five kinds of elementary functions or pH–rate profile fragments to be considered in the analysis of two intersecting profiles. Fig. 1 summarizes these diagramatically. The number of possible interactions between these fragments may be conveniently summarized as a matrix as shown in Table 2. There are in total 60 possible interactions. The kinds of interactions fall into the following categories: crossings, partial or complete overlap, and no overlap. Table S1 enumerates diagramatically all possible interactions between two pH–rate profiles. Furthermore, for every instance involving one point of crossing between profiles there also exists a possible avoided crossing at that point. From Table S1 there are 20 situations involving a crossing at one point and two situations involving two points of crossing. Fig. 2 illustrates two pairs of intersecting pH–rate profiles exhibiting a crossing and an avoided crossing situation, respectively.

Suppose we are given a graph showing two pH–rate profiles where each is associated with a rate constant in the two step consecutive reaction sequence. There are two questions which must be answered sequentially: (i) if there is a region of intersection between the profiles, does the intersection represent a crossing or an avoided crossing? and (ii) which profile corresponds to which step in the reaction? The answer to the first question will determine the functional forms of the pH-profiles, and hence it is immediately obvious why this question must be answered first. Once the functional forms are known then the rate constant–reaction step correspondence may be addressed. Since k_1 and k_2 are both functions of pH, the observation that

Table 1 List of elementary pH–rate profile functions and their derivatives[a]

Mode of catalysis	Function in terms of $[H^+]$, $k_{obs} = f([H^+])$	Function in terms of pH, $\log(k_{obs}) = f(pH)$	Derivative function in terms of pH, $\frac{df}{d(pH)}$	Limiting slopes of $f(pH)$
No catalysis	k_0	$\log k_0$	0	0
Acid catalysis	$k_{H^+}[H^+]$	$\log k_{H^+} - pH$	-1	-1
Acid catalysis with uncatalyzed component	$k_0 + k_{H^+}[H^+]$	$\log(k_0 + k_{H^+}10^{-pH})$	$-\frac{k_{H^+}10^{-pH}}{k_0 + k_{H^+}10^{-pH}}$	-1
Base catalysis	$k_{OH^-}[OH^-] = \frac{k_{OH^-}Q_w}{[H^+]}$	$\log(k_{OH^-}Q_w) + pH$	1	1
Base catalysis with uncatalyzed component	$k_0 + \frac{k_{OH^-}Q_w}{[H^+]}$	$\log(k_0 + k_{OH^-}Q_w 10^{pH})$	$\frac{k_{OH^-}Q_w 10^{pH}}{k_0 + k_{OH^-}Q_w 10^{pH}}$	1
Base catalysis with saturation	$\frac{Q_a k_0}{Q_a + [H^+]}$	$\log(Q_a k_0) - \log(Q_a + 10^{-pH})$	$\frac{10^{-pH}}{Q_a + 10^{-pH}}$	1, at low pH 0, at high pH
Acid catalysis with saturation	$\frac{Q_a k_{H^+}[H^+]}{Q_a + [H^+]}$	$\log(Q_a k_{H^+}) + \log\left(\frac{10^{-pH}}{Q_a + 10^{-pH}}\right)$	$-\frac{Q_a}{Q_a + 10^{-pH}}$	0, at low pH -1, at high pH

[a] The following definitions have been used: $pH = -\log[H^+]$; $Q_w = [H^+][OH^-] = 10^{-14}$; Q_a represents an equilibrium constant equal to concentration quotient; k_0/s^{-1}, $k_{H^+}/M^{-1}\,s^{-1}$, and $k_{OH^-}/M^{-1}\,s^{-1}$ are the uncatalyzed, and acid and base catalytic coefficients, respectively.

Table 2 Matrix representing the number of possible interactions between pH–rate profile fragments[a]

	5	4	4	5	3
		5	5	4	3
			5	4	3
				5	3
					2

[a] Since the matrix is symmetrical about the diagonal only the upper triangular part of the matrix is shown.

these rate constants cannot be unambiguously assigned to the reaction steps may be translated into the statement that the pH-profiles cannot be unambiguously assigned to the reaction steps. This ambiguity may be overcome as described before[4] by recording the variation of the absorption extremum of the kinetic signal involving intermediate *B* with pH and matching this experimental result to either one of the two possible corresponding variations found by simulation. The rate constants k_1 and k_2 are of course found from nonlinear regression analysis of decay, growth, growth-decay, or decay-growth curves.

Distinguishing crossings from avoided crossings ‡

The most effective way to distinguish between these types of crossings is by chemical intuition or knowledge of the reactivity of the chemical species in question. This may be known from other independent experiments performed on the same system or from comparisons with kinetic data from analogous chemical systems. However, when there is no prior chemical

‡ The terms "crossing" and "avoided crossing" used here refer to whether or not the pH–rate profiles intersect. They are not to be confused with their usage in the context of potential energy surfaces.

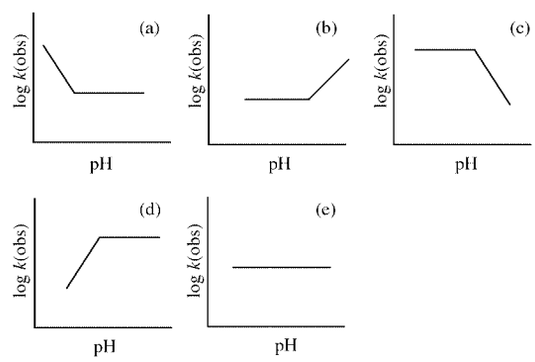

Fig. 1 Summary of pH–rate profile fragments: (a) acid catalysis with uncatalyzed component; (b) base catalysis with uncatalyzed component; (c) acid catalysis with saturation; (d) base catalysis with saturation; and (e) uncatalyzed component.

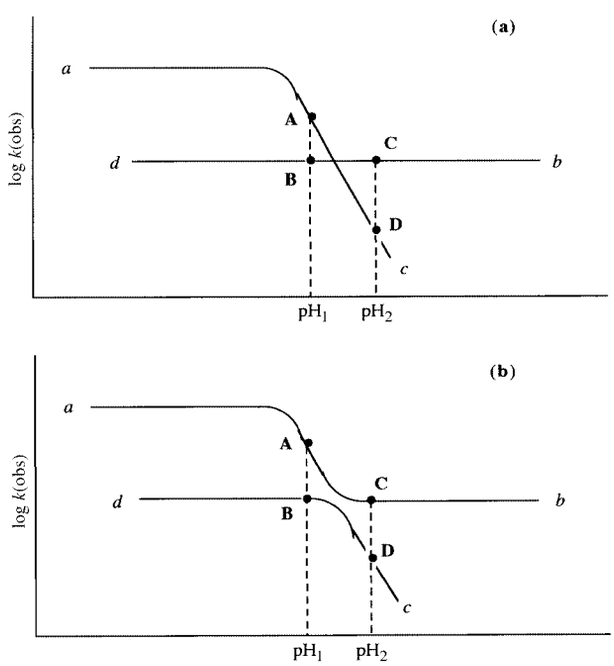

Fig. 2 pH–Rate profile intersections: (a) crossing, and (b) avoided crossing.

knowledge available on a given chemical system obeying a mechanism depicted by Scheme 1, it is still possible to decide the nature of the crossing of the pH–rate profiles provided that this crossing occurs at a point where both legs of the profiles are linear and not curving. This is achieved experimentally by conducting kinetic solvent isotope effect experiments at points on either side of the point of intersection along the lines joining the points of measurement. It is well documented that kinetic solvent isotope effect experiments have proved to be extremely powerful in deciding which mechanism may be operative in a given reaction.[6,7] For the purposes of such experiments the following rules apply to intersecting linear segments:

Rule 1. *If the kinetic solvent isotope effects measured in a region immediately before and immediately after the point of intersection match along a line joining the two points of measurement, and if the corresponding pair of isotope effects match along the other line joining this second pair of points, then the point of intersection is a crossing.*

Rule 2. *If there is a mismatch in kinetic solvent isotope effect values in at least one of the pairs of experiments performed in regions immediately before and immediately after the point of intersection along the line joining the points of measurement, then that point of intersection is an avoided crossing.*

The diagrams in Table S1 depicting intersections between two pH–rate profiles show three possible types of intersections of two linear segments. These pairs may be conveniently enumerated in terms of the slopes of the lines: (a) zero-plus one; (b) zero-minus one; and (c) plus one-minus one. Mechanistically, this experiment will decide which parts of the pH-profiles belong together, and hence which parts of the pH–rate profile correspond to the same chemical species in the reaction. In practice a pair of acid concentrations is selected before and after the point of intersection and the pseudo first order rate constants in normal and heavy water are measured in each case with the condition that $[H^+] = [D^+]$. A key assumption in implementing this analysis is that the form of the kinetic trace in normal water is the same as that in heavy water; that is, if the observed kinetic trace in H_2O is a growth-decay curve then the corresponding observed trace in D_2O will also be a growth-decay curve. Hence, for each of the two acid concentrations examined the isotope effect on the fast component (growth part) of the growth-decay curve is recorded and the corresponding effect on the slow component (decay part) of the trace is also recorded. A point of caution in applying the above two rules is that the point of intersection between pH–rate profiles in normal water occurs in general at a pH different from that in heavy water. This means that the occurrence of intersecting linear segments of pH–rate profiles in normal water does not guarantee that the intersection will also involve linear segments in heavy water. Such a situation has been documented in our previous work on the hydration of fluorenylideneketene in deuterated and non-deuterated aqueous perchloric acid solutions.[5] In normal water the intersection occurred along the straight portions of lines of slope zero and slope minus one; however, in heavy water the intersection occurred at a point that was well into the curved saturation region of the profile corresponding to acid catalysis. Hence, for these rules to be valid the intersection of pH–rate profiles in normal water must involve linear segments. Although this represents a limitation on the applicability of the two rules they are nevertheless useful in supporting a reaction mechanism especially when taken together with other chemical information about a system.

Figs. 2a and b provide an illustrative example of the application of these rules to two pH-rate profiles whose intersection may be a crossing or an avoided crossing. This case depicts an intersection of linear segments of slope zero and slope minus one. In Fig. 2a representing a crossing, legs labelled *a* and *c* belong together and legs labelled *b* and *d* belong together. The corresponding dependencies of the rate constants on hydronium ion concentration have the forms $k = \frac{Q_a k_{L^+}[L^+]}{Q_a + [L^+]}$ and $k = k_0$ for leg pairs *a* and *c*, and *b* and *d*, respectively. The kinetic trace recorded at pH_1 has a fast component (point A) and a slow component (point B). Similarly, points C and D represent the fast and slow components of the kinetic trace recorded at pH_2. A crossing of these pH–rate profiles means that $\left(\frac{k_H}{k_D}\right)_A = \left(\frac{k_H}{k_D}\right)_D$ and $\left(\frac{k_H}{k_D}\right)_B = \left(\frac{k_H}{k_D}\right)_C$. The kinetic solvent isotope effect along leg *db* will then be constant over the acid concentration range and will have a value given by the expression $\frac{k_H}{k_D} = \frac{k_0^H}{k_0^D}$. The magnitude of the ratio is predicted to be small (in the range 3 to 4) owing only to uncatalyzed contributions.[6,7] Similarly, the kinetic solvent isotope effects at points A and D will be equal in magnitude. Since these points lie on the linear portion of the profile showing acid catalysis where $Q > [L^+]$, the value of the isotope effect will be given by $\frac{k_H}{k_D} = \frac{k_{H^+}[H^+]}{k_{D^+}[D^+]} = \frac{k_{H^+}}{k_{D^+}}$ when $[H^+] = [D^+]$.

In Fig. 2b representing an avoided crossing, legs labelled *a* and *b* belong together and legs labelled *c* and *d* belong together. Note that the spatial correspondence of the profiles drawn in Fig. 2b is identical to that in Fig. 2a except that the lines are connected differently. The corresponding dependencies of the rate constants on hydronium ion concentration are of the forms $k = \frac{Q_a k_{L^+}[L^+]}{Q_a + [L^+]} + k_0'$ and $k = \frac{Q_a' k_{L^+}[L^+]}{Q_a' + [L^+]}$ for leg pairs *a* and *b*, and *c* and *d*, respectively. A mismatch in kinetic solvent isotope effect measurements may be predicted in this case if measurements are compared along leg *db*. An avoided crossing between these pH–rate profiles means that $\left(\frac{k_H}{k_D}\right)_B \neq \left(\frac{k_H}{k_D}\right)_C$ and $\left(\frac{k_H}{k_D}\right)_A = \left(\frac{k_H}{k_D}\right)_D$. The left hand side of the avoided crossing (point B) corresponds to an acid catalyzed component that has reached saturation ($Q < [L^+]$) and so the kinetic solvent isotope effect in this region is given by the expression $\frac{k_H}{k_D} = \frac{Q_a'^H k_{H^+}}{Q_a'^D k_{D^+}}$. The right hand side of the avoided crossing (point C), however, corresponds to an uncatalyzed region and so the corresponding effect here is given by the expression $\frac{k_H}{k_D} = \frac{k_0'^H}{k_0'^D}$. The former ratio is predicted to be significantly larger in magnitude than the latter owing to the contribution of the ionization constant to the solvent isotope effect.[6,7]

Absorbance extremum method

Once the functional forms of the two pH–rate profiles are sorted out then the absorbance extremum method may be employed to assign the rate constants to their respective steps in the reaction. The two functions that need to be compared in the absorbance extremum method when the intermediate *B* is monitored uniquely are given by eqn. (3) and (4), where

$$A_B^{max} = A_A^0\left(\frac{\varepsilon_B}{\varepsilon_A}\right)\left(\frac{f}{g-f}\right)\left[\left(\frac{g}{f}\right)^{-f/(g-f)} - \left(\frac{g}{f}\right)^{-g/(g-f)}\right] \quad (3)$$

$$A_B^{max} = A_A^0\left(\frac{\varepsilon_B}{\varepsilon_A}\right)\left(\frac{g}{f-g}\right)\left[\left(\frac{f}{g}\right)^{-g/(f-g)} - \left(\frac{f}{g}\right)^{-f/(f-g)}\right] \quad (4)$$

A_B^{max} is the maximum absorbance of *B*, A_A^0 is the initial absorbance of *A* at time zero, ε_A and ε_B are the absorption coefficients of *A* and *B*, and *f* and *g* are functions of $[H^+]$. In eqn. (3), *f* and *g* correspond to the case $k_1 = f([H^+])$ and $k_2 = g([H^+])$; that is, *f* is associated with the first step in the reaction and *g* is associated

with the second. In eqn. (4), f and g correspond to the case $k_1 = g([H^+])$ and $k_2 = f([H^+])$; that is, f is associated with the second step in the reaction and g is associated with the first. The absorption maxima are obtained from nonlinear least squares fits of the growth-decay curves to expressions of the form eqn. (5) compatible with eqn. (3), where

$$y = a[e^{-k_2 t} - e^{-k_1 t}] \quad (5)$$

$a = A_A^0\left(\frac{\varepsilon_B}{\varepsilon_A}\right)\left(\frac{k_1}{k_1 - k_2}\right) = A_A^0\left(\frac{\varepsilon_B}{\varepsilon_A}\right)\left(\frac{f}{g - f}\right)$; or eqn. (6) com-

$$y = a[e^{-k_1 t} - e^{-k_2 t}] \quad (6)$$

patible with eqn. (4), where $a = A_A^0\left(\frac{\varepsilon_B}{\varepsilon_A}\right)\left(\frac{k_2}{k_2 - k_1}\right) = A_A^0\left(\frac{\varepsilon_B}{\varepsilon_A}\right)\left(\frac{g}{f - g}\right)$.

For all other kinetic traces involving any combination of chemical species including the intermediate B the corresponding pair of equations is eqn. (7) and (8). The definitions

$$A^{\max} = a\left(\frac{bg}{af}\right)^{-f/(g-f)} - b\left(\frac{bg}{af}\right)^{-g/(g-f)} + c \quad (7)$$

$$A^{\max} = a\left(\frac{bf}{ag}\right)^{-g/(f-g)} - b\left(\frac{bf}{ag}\right)^{-f/(f-g)} + c \quad (8)$$

of the parameters a, b, and c are dependent on the combination of chemical species monitored together, and a and b are also functions of f and g.[4] For example, if the reactant, intermediate, and product are monitored simultaneously at a given wavelength, then the definitions $a = A_A^0\left[1 + \frac{g\varepsilon_C - f\varepsilon_B}{\varepsilon_A(f-g)}\right]$, $b = A_A^0\left[\frac{f(\varepsilon_C - \varepsilon_B)}{\varepsilon_A(f-g)}\right]$, and $c = A_A^0\left(\frac{\varepsilon_C}{\varepsilon_A}\right)$ are compatible with eqn. (7); and the definitions $a = A_A^0\left[1 + \frac{f\varepsilon_C - g\varepsilon_B}{\varepsilon_A(g-f)}\right]$, $b = A_A^0\left[\frac{g(\varepsilon_C - \varepsilon_B)}{\varepsilon_A(g-f)}\right]$, and $c = A_A^0\left(\frac{\varepsilon_C}{\varepsilon_A}\right)$ are compatible with eqn. (8). The numerical values of a, b, and c are obtained from nonlinear least squares fits to an expression of the form eqn. (9), where $k_1 = f([H^+])$ and $k_2 = g([H^+])$ are applicable to eqn. (7) and $k_1 = g([H^+])$ and $k_2 = f([H^+])$ are applicable to eqn. (8).

$$y = ae^{-k_1 t} - be^{-k_2 t} + c, \quad (9)$$

The pairs of equations (3) and (4), and (7) and (8) may be applied to any two pH–rate profiles interacting in any of the situations itemized in Table S1. The functional forms of $A_B^{\max}$ or $A^{\max}$ on $[H^+]$ will be very different and hence easily distinguishable upon transposition of rate constants. More precisely, the two possible variations of $A_B^{\max}$ or $A^{\max}$ with $[H^+]$ are related by opposite concavities; that is, the functions are graphically related by a reflection in the $[H^+]$ axis.

Note that if two pH-profiles completely overlap, then we have the trivial situation in which both rate constants have identical dependencies on $[H^+]$ and are hence equally valued. Transposition of rate constants, then, does not cause any difference in the absorption extremum variation with $[H^+]$ and so there is no ambiguity in assigning rate constants to the appropriate reaction step for this trivial situation.

Experimental verification

As in the previous investigation, fluorenylideneketene was generated flash photolytically from 10-diazophenanthren-9(10*H*)-one in aqueous perchloric acid solutions. A transient signal

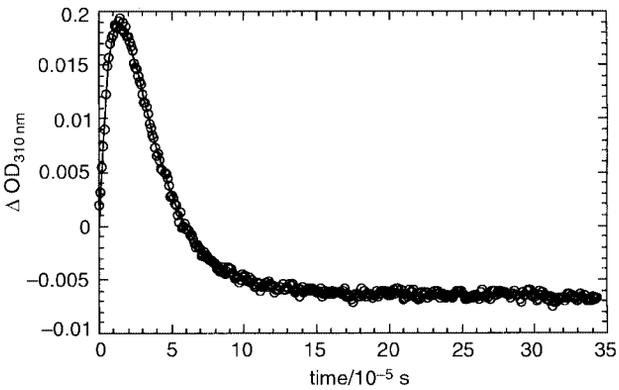

Fig. 3 Growth-decay kinetic trace obtained from flash photolysis of 10-diazophenanthren-9(10*H*)-one at 248 nm in aqueous perchloric acid solution ($[HClO_4] = 0.000795$ M).

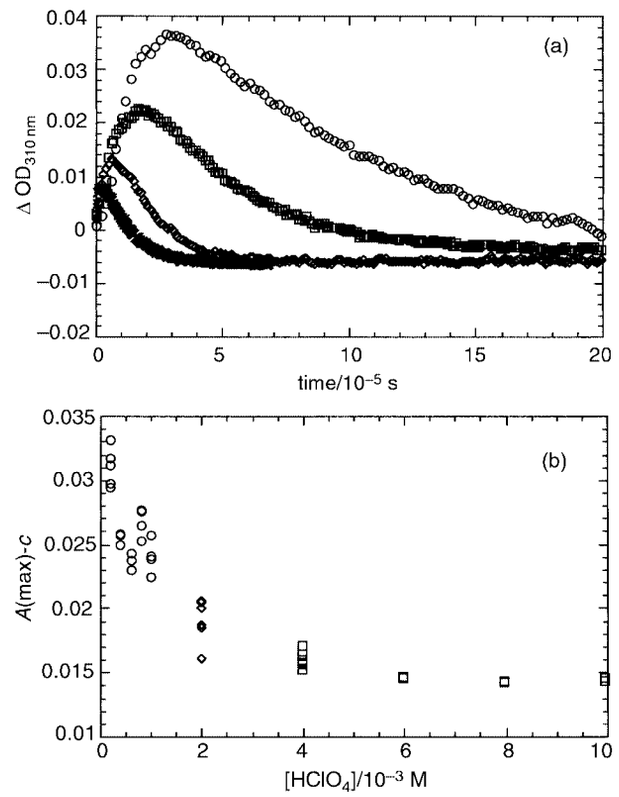

Fig. 4 (a) Variation of growth-decay traces obtained from flash photolysis of 10-diazophenanthren-9(10*H*)-one with perchloric acid concentration: ○, 0.000199 M; □, 0.0004 M; ◇, 0.002 M; ×, 0.00994 M. (b) Relationship between signal amplitude of growth-decay traces recorded from flash photolysis of 10-diazophenthren-9(10*H*)-one and perchloric acid concentration; ○, signals obtained at $[H^+] < 0.002$ M; ◇, signals obtained at $[H^+] = 0.002$ M; □, signals obtained at $[H^+] > 0.002$ M.

observed at 310 nm exhibited typical growth-decay behaviour as would be expected for intermediate B in Scheme 1. An example kinetic trace is shown in Fig. 3. Since it is not possible from this experiment to know whether the observed signals corresponded uniquely to enol intermediate, kinetic traces were fitted to the general expression given by eqn. (9). The results of the non-linear least squares fitting of the data are summarized in Table 3. Note that the descriptors k_1 and k_2 used in the table are arbitrary variable labels and that the subscripts 1 and 2 are not to be associated with steps 1 and 2 in the reaction sequence. In accordance with a previous analysis of growth-decay curves,[4] it is observed that the rate constant k_2 corresponds to the growth part of the trace since it is always larger in magnitude than k_1 and is associated with a negative pre-exponential factor. Included in Table 3 are estimates of the times at which the signals reach their maximum intensities

Table 3 Raw rate data corresponding to fit according to growth-decay expression given by eqn. (9)

$[HClO_4]$/M	a	$k_1/10^4\ s^{-1}$	b	$k_2/10^4\ s^{-1}$	c	$t_{max}{}^a$/μs	$A^{max} - c^b$
0.000199	0.0510	1.20	0.0474	6.80	−0.00436	29.6	0.0295
	0.0442	1.00	0.0355	9.50	−0.00598	23.9	0.0311
	0.0491	1.03	0.0384	8.33	−0.00635	25.3	0.0332
	0.0432	1.06	0.0357	9.39	−0.00457	23.9	0.0297
	0.0481	1.09	0.0386	8.25	−0.00484	25.2	0.0317
0.0004	0.0565	2.77	0.0506	9.79	−0.00427	16.4	0.0257
	0.0641	2.91	0.059	8.80	−0.00383	17.4	0.0259
	0.0496	2.64	0.0423	10.8	−0.00369	15.3	0.0250
0.000599	0.0891	4.44	0.0823	8.93	−0.00546	13.8	0.0243
	0.0725	4.32	0.0644	10.0	−0.00510	12.7	0.0238
	0.086	4.66	0.0749	8.75	−0.00486	12.0	0.0230
	0.0736	4.33	0.0619	9.08	−0.00528	11.9	0.0230
0.000795	0.079	4.33	0.0689	10.1	−0.00654	12.3	0.0265
	0.0842	4.24	0.0779	9.30	−0.00641	14.0	0.0253
	0.0786	3.96	0.0666	9.54	−0.00710	12.8	0.0277
	0.11	4.63	0.0978	8.44	−0.00689	12.7	0.0276
0.000998	0.156	6.00	0.144	8.49	−0.00597	10.7	0.0240
	0.16	6.20	0.148	8.66	−0.00550	10.4	0.0238
	0.115	6.12	0.107	9.84	−0.00503	10.8	0.0224
	0.15	6.12	0.144	9.46	−0.00636	11.8	0.0257
0.002	0.0651	8.14	0.0572	16.3	−0.00580	6.9	0.0185
	0.171	10.9	0.166	13.7	−0.00318	7.1	0.0161
	0.0566	6.64	0.0468	16.2	−0.00588	7.3	0.0205
	0.153	8.25	0.14	10.9	−0.00601	7.2	0.0206
	0.157	8.55	0.145	11.2	−0.00561	7.2	0.0201
	0.094	9.00	0.0841	14.1	−0.00383	6.6	0.0187
0.00398	0.0263	8.21	0.0169	37.8	−0.00620	3.7	0.0152
	0.0273	8.36	0.0178	40.2	−0.00610	3.6	0.0160
	0.0311	8.50	0.0237	32.4	−0.00642	4.5	0.0157
	0.0278	7.61	0.0148	36.1	−0.00710	3.3	0.0171
	0.028	8.25	0.0157	35.5	−0.00637	3.2	0.0165
	0.0268	8.13	0.0149	34.6	−0.00639	3.3	0.0157
0.00596	0.0302	9.72	0.0225	33.8	−0.00608	4.0	0.0147
	0.0261	9.15	0.0141	33.0	−0.00618	2.8	0.0146
0.00795	0.0218	8.83	0.00996	44.5	−0.00616	2.3	0.0142
	0.0205	8.63	0.0118	67.7	−0.00598	2.6	0.0144
0.00994	0.0224	8.94	0.00953	42.0	−0.00683	2.1	0.0146
	0.0206	8.87	0.0118	68.5	−0.00639	2.5	0.0144

[a] The time corresponding to when the kinetic signal reaches its maximum absorption is found from eqn. (10). [b] The value of the maximum absorbance is found from eqn. (11).

and the corresponding signal amplitudes. These quantities are determined from expressions (10) and (11). Figs. 4a and 4b

$$t_{max} = \frac{1}{k_2 - k_1} \ln\left(\frac{bk_2}{ak_1}\right) \quad (10)$$

$$A^{max} - c = ae^{-k_1 t_{max}} - be^{-k_2 t_{max}} \quad (11)$$

show the dependence of signal size on perchloric acid concentration and Fig. 5 shows the respective pH–rate profiles that may be constructed from the rate data.

Avoided crossing *versus* crossing

From the pH-profiles shown in Fig. 5 it is observed that the region of intersection occurs around 0.002 M perchloric acid. The following two pieces of evidence support the assignment of this intersection as a crossing. As argued previously[5] hydration of aromatic ketenes is very weakly catalyzed by acid; whereas, the ketonization of carboxylic acid enols is strongly catalyzed by acid and shows saturation behaviour at high acid concentrations. Hence, based on these observations alone it is reasonable to conclude that the expected pH-profiles corresponding to these behaviours in dilute acidic solution ($[H^+] < Q_a^E$, where Q_a^E is the concentration quotient for the ionization of the enol as an oxygen acid) are a profile of slope zero and another of slope minus one, respectively. Secondly, the kinetic solvent isotope effect for the hydration of fluorenylideneketene in aqueous perchloric acid solution is constant over the range 0.0001–0.01 M $LClO_4$ at an average value of 1.38. This result is typical of

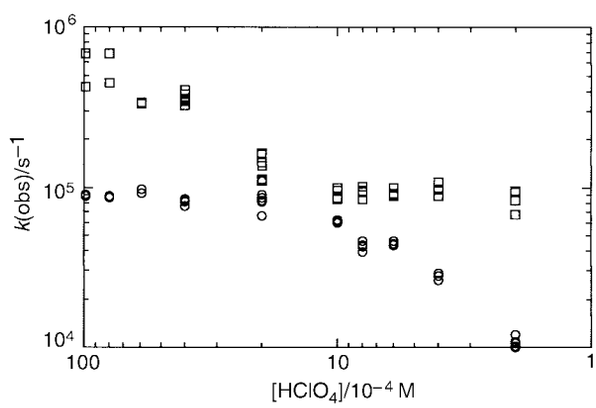

Fig. 5 pH–Rate profiles obtained from rate data obtained from fitting growth-decay kinetic traces to eqn. (9): ○, k_1 rate constant parameter; □, k_2 rate constant parameter.

ketene hydration reactions.[8] Corresponding experiments carried out for the ketonization of fluorene-9-carboxylic acid enolate at concentrations of acid on either side of 0.002 M $LClO_4$ also show consistent kinetic isotope effects. Tables 4 and 5 summarize all of the relevant kinetic solvent isotope effect data. From these experimental evidences it can be concluded that the data points in Fig. 5 can be connected as suggested by Fig. 2a.

Having established the intersection of the profiles as a crossing, the functional forms of the pH–rate profiles are then given by eqn. (12) and (13) for $[H^+] < Q_a^E$. Fitting the appropriate

Table 4 Kinetic solvent isotope effect data for the hydration of fluorenylideneketene in aqueous perchloric acid solution at 25 °C[a]

$[LClO_4]$/M	$k_{obs}/10^4$ s^{-1}, L = H	$k_{obs}/10^4$ s^{-1}, L = D	k_H/k_D
0.00011	11.1, 9.90	8.28, 8.13	1.28 ± 0.07
0.00106	15.8, 12.9, 13.3	8.45, 8.68	1.63 ± 0.11
0.0051	10.6, 10.6, 10.6	7.20, 7.53	1.44 ± 0.03
0.010	8.25, 8.40	7.24, 7.21	1.15 ± 0.01

[a] Ionic strength = 0.10 M ($NaClO_4$).

Table 5 Kinetic solvent isotope effect data for the ketonization of fluorene-9-carboxylic acid enolate in aqueous perchloric acid solution at 25 °C[a]

$[LClO_4]$/M	$k_{obs}/10^4$ s^{-1}, L = H	$k_{obs}/10^4$ s^{-1}, L = D	k_H/k_D
0.00106	12.0, 10.1, 9.53	3.90, 4.11	2.62 ± 0.19
0.0030	36.1, 31.3, 32.1, 31.7	10.2, 10.2	3.22 ± 0.11

[a] Ionic strength = 0.10 M ($NaClO_4$).

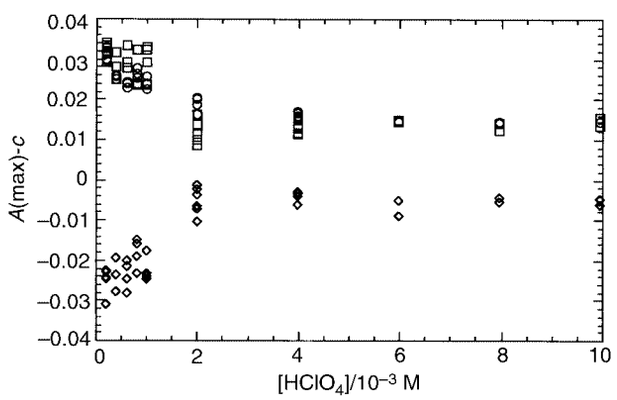

Fig. 6 Relationship between signal amplitude of growth-decay traces recorded from flash photolysis of 10-diazophenanthren-9(10*H*)-one and perchloric acid concentration: ○, experimental data; □, simulated data using eqn. (7) with $k_1 = 5.43 \times 10^7$ [H$^+$] and $k_2 = 8.96 \times 10^4$ for [H$^+$] < 0.002 M, and $k_1 = 8.96 \times 10^4$ and $k_2 = 5.34 \times 10^7$ [H$^+$] for [H$^+$] > 0.002 M; ◇, simulated data using eqn. (8) with $k_1 = 8.96 \times 10^4$ and $k_2 = 5.43 \times 10^7$ [H$^+$] for [H$^+$] < 0.002 M, and $k_1 = 5.43 \times 10^7$ [H$^+$] and $k_2 = 8.96 \times 10^4$ for [H$^+$] > 0.002 M.

$$f = k_{obs} = k_0 \quad (12)$$

$$g = k_{obs} = k'_{H^+}[H^+] \quad (13)$$

observed first-order rate constants shown in the pH-profiles in Fig. 5 to eqn. (12) and (13) yields the following results for the parameters: $k_0 = (8.96 \pm 0.20) \times 10^4$ s^{-1} and $k'_{H^+} = (5.43 \pm 0.13) \times 10^7$ M^{-1} s^{-1}. Tables S2 and S3 summarize the results of the data fits. These values are consistent with $k_0 = 1.07 \times 10^5$ s^{-1} and $k'_{H^+} = 1.25 \times 10^8$ M^{-1} s^{-1} obtained previously.[5]

Absorbance extremum method

Fig. 6 shows the dependencies of the signal size on hydronium ion concentration for the case where *f* and *g* are assigned to k_1 and k_2 in eqn. (7), and the case where *f* and *g* are assigned to k_2 and k_1 in eqn. (8), respectively. Tables S4 and S5 give the numerical data corresponding to these figures. It should be pointed out that the rate constant labels used here have the same meaning as in Scheme 1 and are not to be confused with the arbitrary rate constant labels used in the growth-decay data fitting analysis. Also, Fig. 6 shows the superposition of these

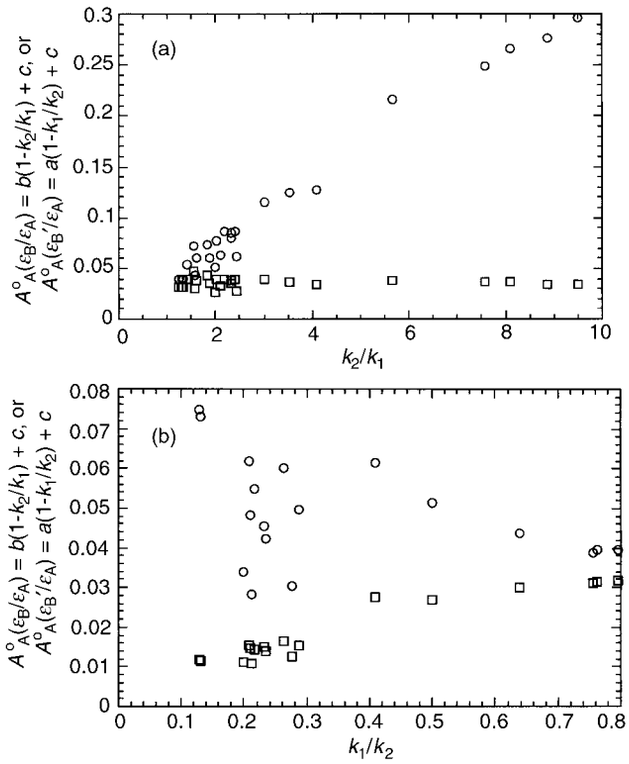

Fig. 7 (a) Relationships between $b\left(1 - \frac{k_2}{k_1}\right) + c$ and $\frac{k_2}{k_1}$ for [$HClO_4$] < 0.002 M (○), and between $a\left(1 - \frac{k_1}{k_2}\right) + c$ and $\frac{k_2}{k_1}$ for [$HClO_4$] < 0.002 M (□). (b) Relationships between $a\left(1 - \frac{k_1}{k_2}\right) + c$ and $\frac{k_1}{k_2}$ for [$HClO_4$] > 0.002 M (□), and between $b\left(1 - \frac{k_2}{k_1}\right) + c$ and $\frac{k_1}{k_2}$ for [$HClO_4$] > 0.002 M (○).

graphs with the experimental data (see Fig. 4) thus indicating that the correct assignment of rate constants in Scheme 1 is that k_1 corresponds to *f* and k_2 corresponds to *g*. Hence, the first step in the reaction sequence is associated with the uncatalyzed profile and the second step in the reaction is associated with the acid catalyzed profile showing saturation. Furthermore, with respect to the growth-decay kinetic traces observed, for concentrations of acid less than 0.002 M the growth corresponds to the ketene hydration and the decay to the enol ketonization; whereas, for concentrations of acid greater than 0.002 M the growth corresponds to the enol ketonization and the decay to the ketene hydration.

Absorption coefficient method

The Alcock analysis[3a,5] applied to the data in Table 4 is summarized in Table S6 and in Fig. 7a and 7b. Note that this analysis is based on the arbitrary rate constant designation used in the nonlinear least squares data fits of the kinetic traces to eqn. (9). At concentrations of acid less than 0.002 M a linear dependence on the ratio k_2/k_1 is observed for ε_B and no dependence is observed for ε_B'. The reverse dependence is found for data obtained at acid concentrations greater than 0.002 M. The rate constant–reaction step assignment made from this second type of analysis is consistent with the one stated above from the absorption extremum method. Moreover, the observation that the dependence on the ratio k_2/k_1 reverses at 0.002 M acid is consistent with the previous conclusion that the two pH–rate profiles indeed cross.

Further, an estimate of $A_A^0\left(\frac{\varepsilon_B}{\varepsilon_A}\right)$ corresponding to the correct absorption coefficient of B can be obtained by taking the average value of the ordinates in Fig. 7a and 7b that show no dependence on either rate constant ratio. The result is $(4.30 \pm 0.18) \times 10^{-2}$.

Estimates of absorption coefficient ratios

In order to obtain estimates of $\frac{\varepsilon_B}{\varepsilon_A}$ and $\frac{\varepsilon_C}{\varepsilon_A}$ the following additional parameters need to be known: the initial absorbance of ketene at the monitoring wavelength (A_A^0), the absorbance of diazoketone solution at the monitoring wavelength prior to flash photolysis (A_{preflash}), and the fraction of photoprecursor left after photolysis (φ). Since absorbances of kinetic traces in flash photolysis experiments are measured as difference optical densities (ΔO.D.'s) relative to photoprecursor absorbances, the preflash absorbance is set equal to zero. Hence, for any kinetic trace of a transient relations (14) apply.

$$\Delta\text{O.D.}_{\text{preflash}} = 0 \quad (14a)$$

$$\Delta\text{O.D.}_{\text{postflash}} = A(t)_{\text{transient}} + (\varphi - 1)A_{\text{preflash}} \quad (14b)$$

In all kinetic runs A_{preflash} is measured to be about 0.016 ± 0.005 at 310 nm. The form of $A(t)_{\text{transient}}$ is identical to eqn. (9) except that the trace is translated upward by an amount equal to A_{preflash}. Hence, eqn. (15) applies. Assuming that all

$$A(t)_{\text{transient}} = \Delta\text{O.D.}_{\text{postflash}} - (\varphi - 1)A_{\text{preflash}} = ae^{-k_1 t} - be^{-k_2 t} + c - (\varphi - 1)A_{\text{preflash}} \quad (15)$$

diazoketone has been photolyzed in a single laser pulse we have $\varphi = 0$ and $A_A^0\left(\frac{\varepsilon_C}{\varepsilon_A}\right) = \lim_{t\to\infty} A(t)_{\text{transient}} = c + A_{\text{preflash}} = (1.03 \pm 0.01) \times 10^{-2}$ where an average value of $c = -(5.66 \pm 0.16) \times 10^{-3}$ was calculated from entries in Table 3. Also, the absorbance of ketene prior to photolysis is estimated to be $A_A^0 = a - b + c + A_{\text{preflash}} = (1.98 \pm 0.01) \times 10^{-2}$ where an average value of $a - b + c = (3.76 \pm 0.35) \times 10^{-3}$ was calculated from entries in Table 3. From these data, the following limiting estimates of absorption coefficient ratios can be made for ketene, enol, and carboxylic acid: $\frac{\varepsilon_B}{\varepsilon_A} = 2.18 \pm 0.09$ (minimium) and $\frac{\varepsilon_C}{\varepsilon_A} = (5.20 \pm 0.04) \times 10^{-1}$ (maximum). These results are reasonable since it is expected that the enol should be the strongest absorbing species owing to its high degree of conjugation; whereas, the carboxylic acid product having the least degree of absorbance loses conjugation of the carboxy group with the fluorenyl aromatic ring system. It should be pointed out that ε_B represents a composite absorption coefficient for fluorene-9-carboxylic acid enol which exists in unionised and ionised forms.§ However, since most of the kinetic data on which all of the analyses described in this work were based were collected in a pH range greater than the pK of the enol ionising as an oxygen acid, the main contributor to ε_B is the absorption coefficient of the enolate.

Experimental

Materials

10-Diazophenanthren-9(10H)-one was prepared by treating phenanthrene-9,10-quinone with (*p*-tolylsulfonyl)hydrazine.[9] All other materials were the best available commercial grades.

Kinetics

Kinetics experiments were carried out using a laser flash photolysis setup at McMaster University which has been previously described.[10] A flow system, with no degassing, was employed in which aqueous perchloric acid solutions of varying concentrations were prepared using deionized distilled water. A transient growth-decay signal monitored at 310 nm was produced upon excitation at 248 nm using a KrF excimer laser (Lambda Physik Compex 120, 12–25 ns, 130 mJ pulse^{-1}). Since precise estimates of signal amplitudes as well as rate constants are necessary for these analyses, it was imperative that recorded kinetic traces were consistent in shape and equal in size from shot to shot for each acid concentration. In order to ensure that a constant amount of transient ketene was produced from run to run, two criteria were rigorously met. Firstly, solutions were carefully made up so that each solution had a substrate concentration of 1.45×10^{-5} M. Secondly, the power of the excitation laser pulse, which was recorded for each shot with an internal power meter, remained constant from shot to shot. Five to ten separate signals were signal averaged for each kinetic run and the resultant trace comprised of 400 points was then fitted to a double exponential expression by a nonlinear least squares algorithm using KaleidaGraph software. Time scales were selected as best as possible so that traces had sufficient points collected in the growth and decay regions for best estimates of parameters to be made. At acid concentrations in which it was not possible to select a time base fulfilling this criterion, traces at short and long time scales were first recorded separately, and then joined together and normalized into a single trace before being analyzed. The procedure was as follows. Given trace A recorded at a short time scale with preflash time Δt_A and trace B recorded at a long time scale with preflash time Δt_B, the time data in trace A were translated to match the time zero point of trace B by an amount equal to $\Delta t_B - \Delta t_A$. Since the maximum absorption of trace A is more accurately determined than that of trace B, trace B was normalized to trace A by multiplying the absorption data of trace B by the ratio $\frac{\text{O.D.}_A^{\max}}{\text{O.D.}_B^{\max}}$. The resultant array of data points was then amalgamated into one set of points corresponding to a single trace. This final trace was then offset to zero time by subtracting Δt_B from the time data. All resulting negative valued times in the array from this operation were truncated. Finally, the resultant data points were fitted to appropriate growth-decay expressions as before. All kinetics experiments were performed at 23 °C.

Absorbance measurements

UV absorbances of solutions prior to photolysis were measured in 1.0 cm pathlength quartz cuvettes using an HP 8451A diode array spectrophotometer.

Summary

The absorbance extremum method used to assign rate constants to reaction steps in consecutive reactions has been demonstrated for kinetic schemes involving simultaneous pH–rate profiles. The method is general and is applicable to all possible interactions between pH–rate profiles. Its greatest strength is its resolution of the ambiguity problem for sequential reactions for which additional experimental knowledge may be difficult to implement or for those which have no known analogues for comparison. Moreover, it is shown that deeper mechanistic insights about a chemical reaction may be obtained from collected kinetic traces beyond

§ The composite absorption coefficient ε_B is related to the absorption coefficients of enol, ε_{B_1} and enolate, ε_{B_2}, according to $\varepsilon_B = \varepsilon_{B_1} f_{B_1} + \varepsilon_{B_2} f_{B_2}$, where f_{B_1} and f_{B_2} represent the fractional contributions of fluorene-9-carboxylic acid enol existing in enol and enolate forms; $f_{B_1} = [H^+]/([H^+] + Q_a)$ and $f_{B_2} = Q_a/([H^+] + Q_a)$. A referee is acknowledged for pointing this out.

simply estimating magnitudes of rate constants. Under certain conditions kinetic solvent isotope effect experiments can be used to distinguish crossings from avoided crossings in pH–rate profiles. The hydration of fluorenylideneketene in aqueous perchloric acid solutions is an ideal chemical system for demonstrating and testing the use of the absorbance extremum method. The importance of careful recording of kinetic traces is also emphasised in flash photolysis experiments. Pharmacokineticists, enzymologists, biochemists, and bio-organic chemists will find the method useful and easy to apply in studies of sequential degradations of bioactive molecules in aqueous solution.

Acknowledgements

Natural Science and Engineering Research Council (NSERC) of Canada is gratefully acknowledged for funding the laser flash photolysis facility at McMaster University. J. A. also thanks Professor A. J. Kresge for stimulating discussions regarding this problem and referees for their valuable comments.

References

1 J. R. Keeffe and A. J. Kresge, in *Techniques of Chemistry*, *Vol. VI*, *Investigations of Rates and Mechanisms of Reactions*, ed. C. F. Bernasconi, Wiley-Interscience, New York, 1986, Part 1, Ch. XI.
2 G. M. Loudon, *J. Chem. Educ.*, 1991, **68**, 973.
3 (*a*) N. W. Alcock, D. J. Benton and P. Moore, *J. Chem. Soc.*, *Faraday Trans.*, 1970, **66**, 2210; (*b*) J. H. Espenson, *Chemical Kinetics and Reaction Mechanism*, McGraw-Hill Book Company, New York, 1981; (*c*) A. R. Fersht and W. P. Jencks, *J. Am. Chem. Soc.*, 1970, **92**, 5432; (*d*) A. Fersht, *Enzyme Structure and Mechanism*, W. H. Freeman, New York, 1985.
4 For a detailed discussion of this problem the reader is referred to J. Andraos, *Can. J. Chem.*, 1999, **77**, 565 and references therein.
5 J. Andraos, Y. Chiang, A. J. Kresge and V. V. Popik, *J. Am. Chem. Soc.*, 1997, **119**, 8417.
6 A. J. Kresge, R. A. More O'Ferrall and M. F. Powell, in *Isotopes in Organic Chemistry: Secondary and Solvent Isotope Effects*, eds. E. Buncel and C. C. Lee, Elsevier, New York, 1987, Vol. 7, Ch. 4.
7 J. R. Keeffe and A. J. Kresge, in *The Chemistry of Enols*, ed. Z. Rappoport, Wiley, New York, 1990, pp. 399–480.
8 (*a*) J. Andraos, Y. Chiang, C. G. Huang, A. J. Kresge and J. C. Scaiano, *J. Am. Chem. Soc.*, 1993, **115**, 10605; (*b*) J. Andraos, PhD Thesis, University of Toronto, 1992; (*c*) A. Allen, A. J. Kresge, N. P. Schepp and T. T. Tidwell, *Can. J. Chem.*, 1987, **65**, 1719.
9 (*a*) M. P. Cava, R. L. Litle and D. R. Napier, *J. Am. Chem. Soc.*, 1958, **80**, 2257; (*b*) O. Süs, H. Steppan and R. Dietrich, *Justus Liebigs Ann. Chem.*, 1958, **617**, 20.
10 (*a*) W. J. Leigh, R. Boukherroub and C. Kerst, *J. Am. Chem. Soc.*, 1998, **120**, 9504; (*b*) W. J. Leigh, M. S. Workentin and D. Andrew, *J. Photochem. Photobiol. A: Chem.*, 1991, **57**, 97.

Paper a905324g